Microwave Hyperthermia Performance Analysis of Wideband Dipole Antenna

Yildiz, Gulsah; Aydinalp, Cemanur; Joof, Sulayman; Karacuha, Kamil; Celik, Feza Turgay

DOI
10.1109/MeMeA65319.2025.11068107

Publication date
2025

Document Version
Final published version

Published in
Proceedings of the 2025 IEEE Medical Measurements & Applications (MeMeA)

Microwave Hyperthermia Performance Analysis of Wideband Dipole Antenna

Gulsah Yildiz*, Cemanur Aydinalp*, Sulayman Joof*, Kamil Karacuha*, Feza Turgay Celik†,
*Faculty of Electrical and Electronics Engineering, Istanbul Technical University, Istanbul, Turkiye
†Department of Microelectronics, Delft University of Technology, Delft, Netherlands
gulsahyildiz@itu.edu.tr, aydinalp16@itu.edu.tr, joof@itu.edu.tr, karacuha17@itu.edu.tr, f.t.celik@tudelft.nl

***Abstract*—Hyperthermia (HT) is an adjuvant treatment method aimed at elevating the temperature in target tissues while minimizing the impact on surrounding non-target tissues. Microwave hyperthermia is particularly notable due to the strong interactions between microwaves and biological tissues. The design of a microwave hyperthermia applicator is a critical component of the treatment system, making various antenna designs and arrays a focal point of research in this field. The operating parameters of the designed antenna significantly influence metrics that indicate the efficiency of hyperthermia treatment, such as target-to-body Specific Absorption Rate (SAR) and temperature ratios. In this study, a two-layer hyperthermia applicator utilizing eight microstrip dipole-type antennas with broadside radiation characteristics was proposed. Hyperthermia performance across four different target regions of tissue at 20 frequencies was analyzed. Although this study implemented a simple fat cylinder as a body part, the target-to-body Specific Absorption Rate (SAR) ratios showed that for each target position, a different frequency provided the best performance. Adding the complexity of a real-life problem of an inhomogeneous body with complex geometries, using broadband antennas to perform hyperthermia on different frequencies will provide a significant advantage for focused hyperthermia. The results demonstrate that different frequencies yield varying hyperthermia performance depending on the target position, with mid-range frequencies (2800–3200 MHz) generally providing better SAR distribution and thermal efficiency. Notably, 3000 MHz exhibited the best balance between targeted heating and minimal impact on healthy tissues, while higher frequencies, such as 4000 MHz, resulted in suboptimal performance due to lower realized gain.**

***Index Terms*—Antennas, electromagnetics, propagation, microwave hyperthermia.**

I. Introduction

Focused hyperthermia (HT) is a promising complementary treatment method that selectively targets cancerous tissues by raising their temperature to damage and shrink the cells, thereby causing minimal harm to normal tissues. This process also enhances the susceptibility of some tumor cells to radiation therapy and chemotherapy [1], [2]. The HT method artificially raises tumor temperatures to between 40°C and 45°C, employing various techniques such as ultrasound, thermal conduction, and microwave radiation devices [3]. The final effects of HT can vary for each patient depending on the composition of their tissues (such as fat, fibroglandular, or bone) and the tumor's location. Microwave hyperthermia (MHT) is of great interest due to the strong interactions between microwaves and biological tissues [4]. However, applying MHT for breast cancer presents considerable challenges because of the complex and heterogeneous characteristics of breast tissues. There exists a significant gap in the literature regarding the effective implementation of MHT for breast cancer [5].

Most carcinomas are located in the upper outer quadrant of the breast [6]; however, malignant tissues can also develop in various locations, including deep-seated areas near the chest wall. Consequently, it is essential to manage power deposition profiles to effectively target lesions of different sizes and shapes that may arise in various regions of the breast. MHT utilizes beamforming techniques to direct microwave energy toward the breast tumor by adjusting the excitation phases and amplitudes of the antenna array, influencing heating patterns and therapeutic outcomes. To maximize the benefits of MHT, hyperthermia treatment planning (HTP) must be personalized for each patient. The careful selection of the MHT applicator is a critical step in the HTP process [4]. Furthermore, the effectiveness of hyperthermia treatment is significantly influenced by the electric field distribution produced by microwave antennas. Therefore, the literature includes several studies that have been conducted using different antennas for hyperthermia applications [11], [12], [13], [14], [15]. For instance, in [11], a corner T-slotted antenna was proposed for hyperthermia treatment at 2.45 GHz. The designed antenna achieved an S_{11} of -17.46 dB and a gain of -5.1 dBi. In [12], a slotted circular patch antenna was designed for targeted heating, achieving an S_{11} of -20.9dB at the operating frequency of 2.45 GHz. In [13] study, a single horn antenna operating at 2.45 GHz was tested on hemispherical phantoms with varying densities and tumor sizes for hyperthermia treatment. To minimize reflection, a matched layer (lens) with selected permittivity values (ϵ_{eff} =21 and ϵ_{eff} =16 at 2.45 GHz) was applied to the skin, corresponding to the effective permittivity of breast phantom layers (skin, fat, glandular tissue, and tumor). Simulation and experimental results confirmed that this matching medium effectively increased tumor temperatures for hyperthermia without requiring additional input power. These hyperthermia systems was suggested to use a single antenna for the treatment. The applicator designed was not mentioned as a main issue. These hyperthermia systems were suggested to use a single antenna for treatment, and the applicator (array) design was not highlighted as a primary concern. Apart from these, in [14], nine-element slotted patch antennas and

2025 IEEE Medical Measurements & Applications (MeMeA) | 979-8-3315-2347-3/25/$31.00 ©2025 IEEE | DOI: 10.1109/MEMEA65319.2025.11068107

a numerical breast model with multiple tumors demonstrated their capability to efficiently focus energy on small areas. The proposed antenna achieved an S_{11} better than -47 dB, and simulation results indicated effective tumor heating at 43°C within 10 minutes while maintaining SAR levels within IEEE safety limits. Therefore, the study concluded that efficient use of three-element antennas at lower power levels is a promising possibility. Furthermore, in [15] a multi-resonance applicator is introduced with 35 antenna elements operating in different frequency bands, designed using a hybrid gravitational search and particle swarm optimization algorithm to focus heat precisely on tumor. The multi-resonance applicator demonstrated superior performance compared to a single resonance applicator, effectively elevating tumor temperatures above 42.5°C with 60 watts of microwave power.

In this work, a microstrip dipole-type antenna with broadside radiation characteristics is designed, featuring a reflector positioned behind the antenna layer to increase directivity and focus energy on the target tissue. Since hyperthermia performance is evaluated using target-to-body SAR and temperature ratios, hotspot-to-target SAR and temperature ratios, and the average temperature at healthy tissue, antenna directivity becomes a crucial design parameter for hyperthermia systems. Furthermore, this study examines the feasibility of employing a wideband antenna and utilizing 20 frequencies across four different target regions of tissue to evaluate hyperthermia performance.

II. Material and Methods

The general practice with microwave hyperthermia is to have a single-frequency antenna and apply the energy at that frequency. Each of the antenna needs to be excited by a different power and phase level and multi-frequency excitation with varying parameters is not feasible for the hardware. This study will examine the feasibility of using a wideband antenna and to utilize multiple frequencies to increase the hyperthermia performance.

A. Antenna Design

This section provides a single antenna design and its array configuration. The design employs a microstrip dipole-type antenna for low-profile, broadside radiation with directive characteristics. The reflector behind the antenna layer increases directivity. As there is a balanced to unbalanced transition between antenna and RF excitation, a balun structure is needed. Printed balun is preferred to ease the fabrication process, which is located perpendicular to the antenna plane and reflector structures to eliminate coupling and extra volume necessity [7]. The antenna geometry and dimensions are provided in Figure 1. In Table I, the details about the dimensions are given.

Broadband requirements on the antenna are satisfied by using sectoral dipole sections. The arms of the dipole are flared out, and a wide dipole structure is obtained. A wide antenna surface enables excitation of similar surface currents at different frequencies. Having a similar current distribution

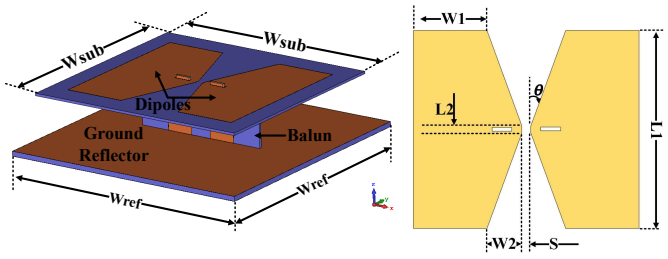

Fig. 1. (a) Isometric view of the antenna and balun complex and (b) top view of the wide dipole.

TABLE I
Dimensions of the Proposed Antenna.

Parameter	Value(mm)	Parameter	Value(mm)
s	2.5	W1	20.35
L1	55	W2	9.6
L2	2	W3	4
L3	17	W4	8
L4	3	W5	4
L5	4	W6	7
L6	5	W7	14
L7	5	W8	6.5
L8	3.5	W9	8
L9	1.81	W10	5
L10	12.4	W11	3.9
L11	2	W12	45
L12	1.3	W13	10
L13	0.3	W14	12
W SUB	76	W17	1
W REF	85	θ(deg)	45

yields broad-band operation regarding the antenna impedance. In addition to that, the wide dipole structure excites all different frequencies at the same plane, resulting in a wide radiation pattern bandwidth. The geometry of the balun structure specialized to feed the dipole antenna design is given in Figure 2. Here, a wideband printed balun designed to bridge the gap between a 50 Ω unbalanced coaxial feedline and a balanced wideband dipole antenna is proposed. The balun plays a crucial role in ensuring efficient power transfer, achieving impedance matching, and suppressing unwanted current modes, all while supporting wideband performance. The design consists of two main layers: a signal plane and a ground plane. The signal plane incorporates several microstrip sections with varying widths and lengths to gradually transform the impedance across the target frequency range. This stepped impedance configuration is key to the balun's ability to handle a wide bandwidth. The ground plane, on the other hand, features carefully designed slots and cutouts. These elements guide current distribution and enhance coupling, ultimately improving the overall performance of the balun [8]. A wideband dipole antenna combined with a wideband balun results in matching between 2.2 GHz and 4.4 GHz as can be seen in the scattering (S) parameters of the antenna (see Figure 3). Dimensions and the geometry of the patch dipole play an important role in bandwidth. In Figure 4, the effect of (a) θ and (b) L1 on the $|S_{11}|$ parameter of the dipole antenna

are provided. These figures illustrate that the increase in the width of the flaring region of the dipole increases bandwidth. A similar effect can be observed for the flare angle. The increase on the θ strengthens the second resonance, yielding an increase in the bandwidth. The limit on these measures are determined by the additional capacitive load on the antenna.

After achieving wideband impedance matching with the balun structure, we will investigate the radiation behaviors of the antenna in the operating region. Radiation patterns for different frequencies are given in Figure 5. As can be seen, a stable and almost fixed-gain radiation pattern was obtained in the frequency band. This antenna includes a reflective surface which is beneath the radiating dipole. This reflecting surface blocks back-radiation and results in an increase in the gain which is preferred in imaging problems. In Figure 6, surface currents of thick dipoles are given at various frequencies. As seen in the figure, the current on the metallic surface behaves like a classical dipole current for wide frequency band. This yields the dipole radiation characteristics observed in Figure 5.

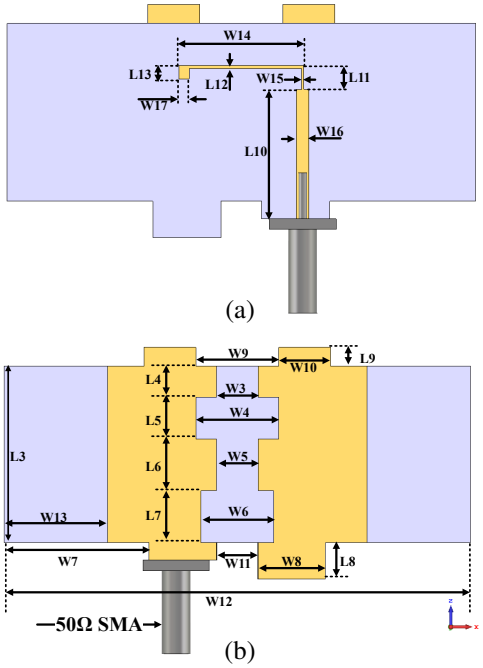

Fig. 2. (a) Ground and (b) signal planes of the Balun structure.

The study uses wide-band dipole antennas in a circularly formed array structure to focus the beam on the center location. The array is formed in a planar fashion; it consists of two layers on the z-axis, and each layer contains four antenna elements. In one layer, antenna elements are located by placing each element 90^0 rotated from each other in the ϕ axis, and the second layer is added by rotating the first layer by 45^0. This unique array formation enables beam scanning in both elevation and azimuth domains to make better beam localization.

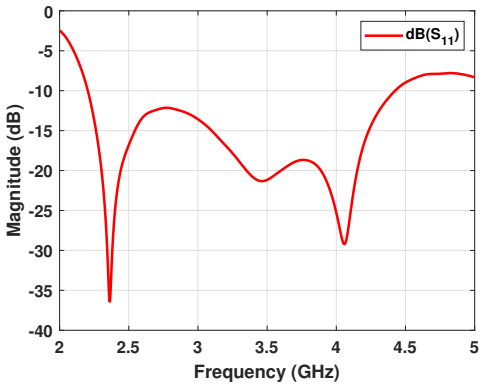

Fig. 3. $|S_{11}|$-parameter of the proposed antenna element in free space.

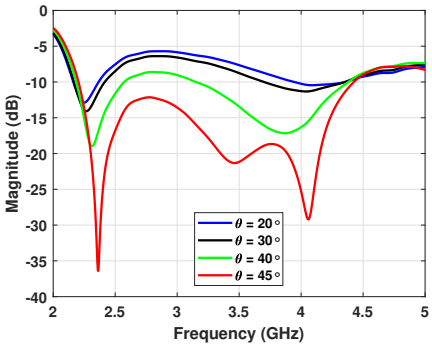

(a)

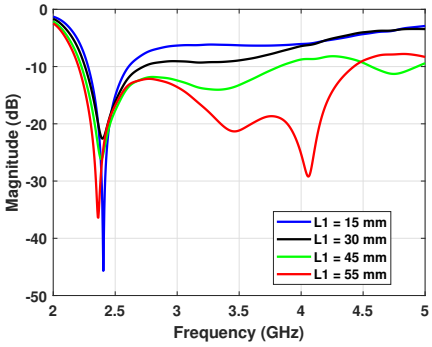

(b)

Fig. 4. Effect of (a) θ and (b) L1 on the $|S_{11}|$ parameter of the dipole antenna in free space.

B. Microwave Hyperthermia

When the i^{th} antenna is excited, the electric field (EF) vector inside the region of interest (ROI) can be shown with $\vec{E}_i$, and α_i represents the excitation magnitude and ϕ_i is the excitation phase. The total EF inside the body formed by eight antennas and the corresponding specific absorption rate (SAR) can be formulated as:

$$\vec{E}_{tot}(r) = \sum_{i=1}^{8} \alpha_i \vec{E(r)}_i e^{j\phi_i} \text{ and } SAR(r) = \frac{0.5\sigma(r)|\vec{E}_{tot}(r)|^2}{\rho(r)} \quad (1)$$

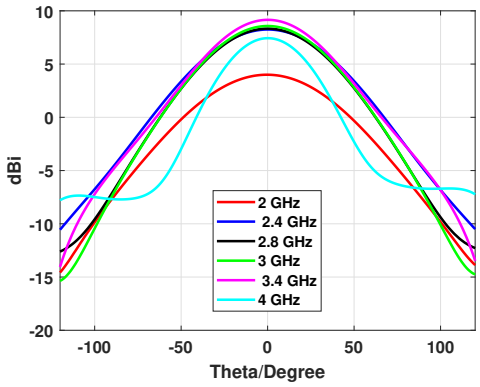

Fig. 5. Radiation pattern of the antenna in free space.

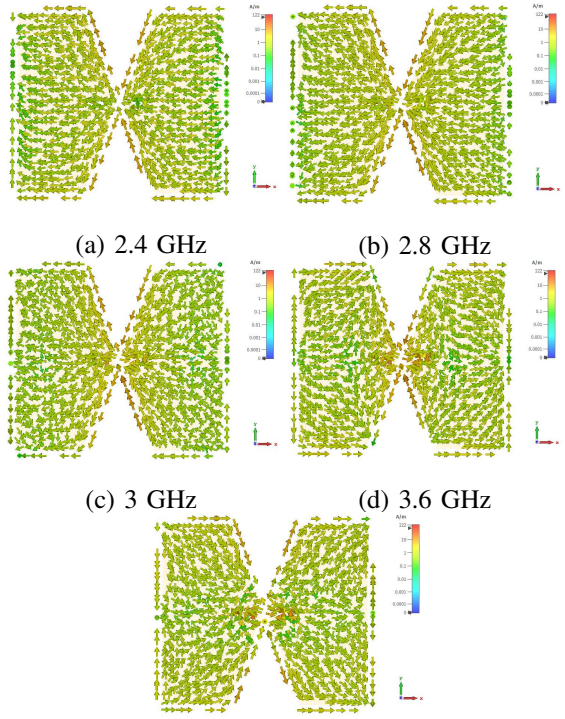

(a) 2.4 GHz (b) 2.8 GHz

(c) 3 GHz (d) 3.6 GHz

(e) 4 GHz

Fig. 6. Surface current of thick dipoles at (a) 2.4 GHz (b) 2.8 GHz (c) 3 GHz (d) 3.6 GHz (e) 4 GHz in free space.

where r is the position vector, σ and ρ are the electrical conductivity (S/m) and the density (kg/m^3) of the body, respectively.

The hyperthermia performance was evaluated by target-to-body SAR and temperature ratios (TBR_S and TBR_T), hotspot-to-target SAR and temperature ratios (HTQ_S and HTQ_T) and the average temperature value at the healthy tissue $avT_{healthy}$ (°C).

$$TBR_S = \frac{avSAR_{target}}{avSAR_{body}} \text{ and } TBR_T = \frac{avT_{target}}{avT_{body}} \quad (2)$$

$$HTQ_S = \frac{avSAR_{hotspot}}{avSAR_{target}} \text{ and } HTQ_T = \frac{avT_{hotspot}}{avT_{target}} \quad (3)$$

$$avT_{healthy} = \frac{\sum_{Healthy\ Region} T}{Area\ of\ Healthy\ Region} \text{°C} \quad (4)$$

where $avSAR_\Omega$ and avT_Ω is the SAR and temperature average at three-dimensional Ω domain. A hotspot is defined as the region with the highest temperature other than the target itself. A detailed explanation can be found in [10].

1) Hyperthermia Applicator System: Eight microstrip dipole-type antennas were positioned in a cylindrical circumference to form the array. The array structure consists of two layers based on the y-direction. In the first layer, four antennas are placed by 90^0 rotated from each other. The distance between antennas that face each other is 200 mm. Due to the cylindrical array formulation, all antennas have an equal distance to the phantom, which is 50 mm. The second layer of the array is positioned 80 mm above the first layer in the y-direction. The second layer also has the same element placement as the first layer, but the elements on this layer are rotated 45^0 regarding the first layer. All the angular placement explained above is done in the xz-plane; therefore, the polarization of the antennas stays linear in the xz-plane. The top and isometric view of the array can be seen in Figure 7.

The antenna excitation magnitude and the phase were optimized using comprehensive-learning particle swarm optimization (cl-PSO) to adjust the parameters such that the energy focus at the desired center is the highest. 40 particles and 1000 iterations were utilized, though the optimization reached saturation after 600 iterations on average. The used cost function for the minimization problem was $cost = avSAR_{healthy} \times HTQ_S/TBR_S$, which was constructed over the SAR distribution. Antenna magnitudes were restricted such that the maximum antenna power was 50 W. The Pennes' bioheat equation [9] can be applied to biological tissues for real-life applications, however in this study, a fat phantom modeled as a cylinder with a radius of 50 mm and a height of 100 mm was utilized. The heat equation was computed to calculate the temperature distribution at a given time, where the initial temperature and the boundary temperature were modeled as 25°C. The hyperthermia was applied until the target center reached 45°C and the hyperthermia duration was reported as a performance metric. The resulting temperature distributions were obtained for selected frequencies and the targets.

III. Results

Twenty frequencies from 2100 MHz to 4000 MHz with 100MHz steps were chosen to be examined. The hyperthermia performance was evaluated for four positions, ([0,0,0] mm, [0,30,0] mm, [0,20,0] mm, [20,0,0] mm). The targets were modeled as 15 mm × 15 mm × 15 mm cubes centered at these points and the healthy regions were modeled as the domain outside of the 19 mm × 19 mm × 19 mm cubes centered at these points. Fig.8(a) illustrates the hyperthermia performance metrics evaluated for the twenty frequencies and the four

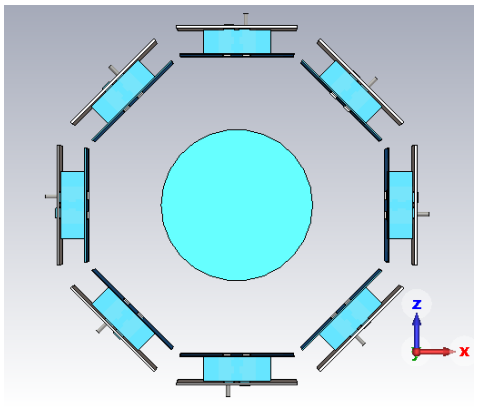

((a))

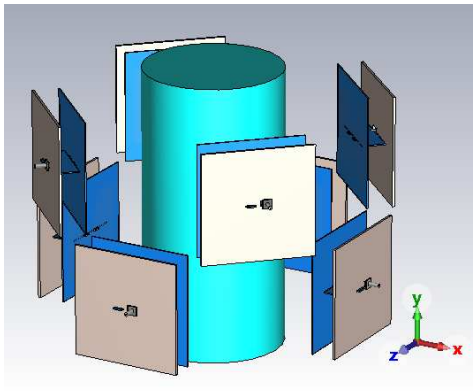

((b))

Fig. 7. Microwave hyperthermia applicator system with eight antennas placed in two layers cylindrically around the cylindrical fat body. (a) Top view, (b) side view of the system.

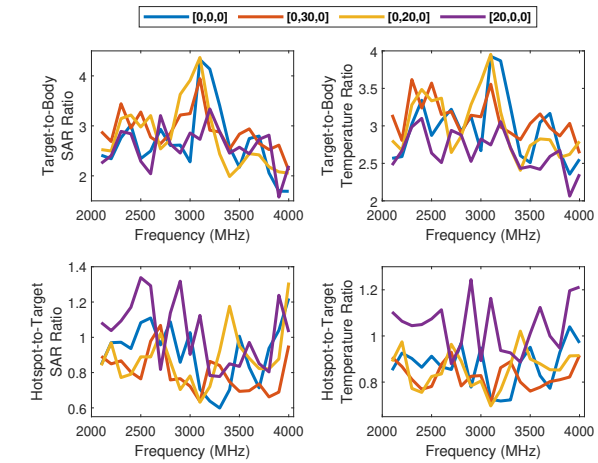

((a))

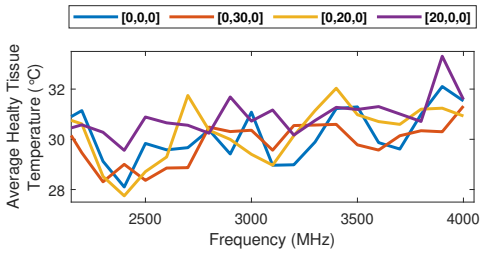

((b))

Fig. 8. Microwave hyperthermia performance metrics for frequencies between 2100 MHz and 4000 MHz evaluated for four target positions.

target positions. Each operating frequency produces a different performance for each target. For example, at [0,0,0] target, the middle frequencies (2800-3200 MHz) produced higher TBR and lower HTQ values, which suggests a better performance. Moreover, lower frequencies deliver higher performance than the higher frequency values. This also holds for other targets with decreasing gravity. Fig.8(b) displays the average temperature at the healthy body domain evaluated for four targets for twenty frequencies. The general trend is that $avT_{healthy}$ increases with increasing frequency.

The optimized SAR for 3000 MHz and the [0,30,0] target, and the corresponding temperature distribution after 11.4 minutes of hyperthermia are shown in Figs. 9. The total antenna input power was 288 W and the highest temperature value was calculated at [-7,35,5] mm as 48.6°C. The hyperthermia metrics were computed as 3.2 for TBR_S, 3.1 for TBR_T, 0.72 for HTQ_S , 0.83 for HTQ_T and 30.4°C for $avT_{healthy}$. For another frequency and target, 2700 MHz and [20,0,0] mm, the optimized SAR and the corresponding temperature distribution after 8.1 minutes of hyperthermia are displayed in Fig.9(c)-9(d). The total antenna input power was 247 W and the highest temperature value was calculated at [11,-1,3] mm as 48.1°C. The hyperthermia metrics were computed as 3.3 for TBR_S, 3.1 for TBR_T, 0.78 for HTQ_S , 0.9 for HTQ_T and 30.2°C for $avT_{healthy}$.

Through the examined frequency range, 4000 MHz produced the worst performance. This may be due to the lower realized gain it has as illustrated in Fig. 5. Furthermore, though 3400 MHz supplies a higher realized gain than 3000 MHz, the HT performance is superior for 3000 MHz. Additionally, 2100 MHz did not yield the worst HT performance although its S_{11} parameter is the worst among the examined frequencies.

IV. Conclusion

HT methods are a valuable adjunctive treatment technique that increases the temperature of target tissues while minimizing the impact on surrounding tissues. Therefore, the performance of microwave hyperthermia applications primarily depends on antenna designs that optimize energy delivery for desired therapeutic outcomes. In this study, we demonstrate the performance analysis of a designed microstrip dipole antenna for microwave hyperthermia applications. By employing a reflector to increase directivity, the antenna effectively focuses energy on targeted tissues while reducing thermal effects on adjacent tissues. Furthermore, the evaluation across multiple frequency ranges and various tissue regions highlights the importance of flexibility for patient-specific treatment and that calls attention to further examination of wideband antenna

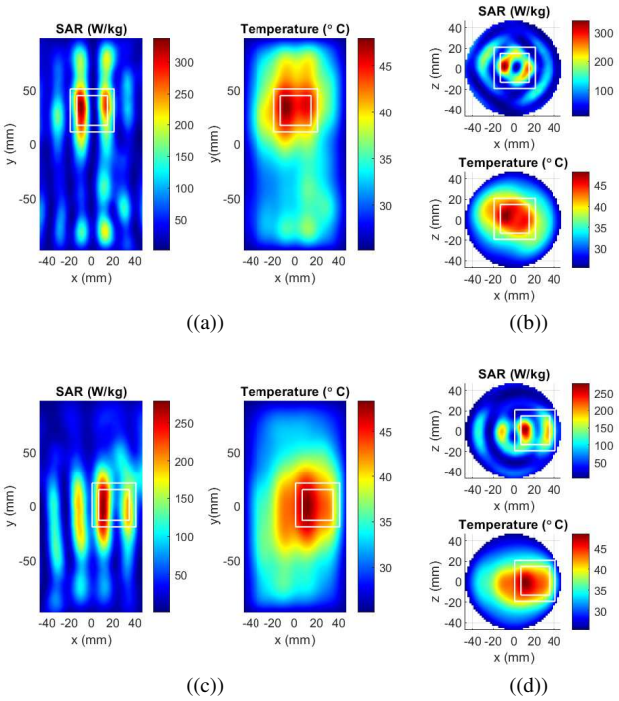

Fig. 9. SAR (W/kg) and temperature (°C) distributions within the body formed during the hyperthermia application; with 3000 MHz frequency, optimized for [0,30,0] target: distributions at (a) $z = 0$ mm and (b) $y = 30$ mm slices, with 2700 MHz frequency, optimized for [20,0,0] target: distributions at (a) $z = 20$ mm and (b) $y = 0$ mm slices. The inner white square represents the position of the target and the outer white square represents the boundary for the healthy tissue

designs in hyperthermia. Future research could explore development in antenna geometry and arrays to improve treatment sensitivity. Consequently, this work can address existing gaps in the literature and challenges associated with developing effective microwave hyperthermia systems.

ACKNOWLEDGMENT

This study was funded by the Scientific Research Unit (BAP) of Istanbul Technical University, Project No. FHD-2024-46417, MGA-2023-45157 and by TUBITAK, Project No. 123N484.

REFERENCES

[1] J. Zee, D. González, G. Rhoon, J. Dijk, W. Putten, and A. Hart, "Comparison of radiotherapy alone with radiotherapy plus hyperthermia in locally advanced pelvic tumours: a prospective, randomised, multicentre trial," *The Lancet*, vol. 355, pp. 1119-1125, 2000.

[2] S. Jha, P. Sharma, and R. Malviya, "Hyperthermia: role and risk factor for cancer treatment," *Achievements in the Life Sciences*, vol. 10, pp. 161-167, 2016.

[3] H. Alexander, "Isolation perfusion," in *Cancer: Principles and Practice of Oncology*, 1st ed. Philadelphia: Lippincott Williams & Wilkins, 2001, pp. 2.

[4] G. Yildiz, I. Farhat, L. Farrugia, J. Bonello, K. Zarb-Adami, C. Sammut, T. Yilmaz, and I. Akduman, "Comparison of microwave hyperthermia applicator designs with for a dipole and connected array," *Sensors*, vol. 23, no. 6592, 2023.

[5] G. Altintas, I. Akduman, A. Janjic, and T. Yilmaz, "A novel approach on microwave hyperthermia," *Diagnostics*, vol. 11, no. 493, 2021.

[6] A. Lee, "Why is carcinoma of the breast more frequent in the upper outer quadrant? A case series based on needle core biopsy diagnoses," *The Breast*, vol. 14, pp. 151-152, 2005.

[7] F. T. Çelik, S. Joof, and K. Karaçuha, "A dual-polarized bandwidth enhanced filtering dipole antenna design for 5G," *IEEE Access*, vol. 11, pp. 78754-78767, 2023.

[8] C. F. Ding, X. Y. Zhang, and M. Yu, "Simple dual-polarized filtering antenna with enhanced bandwidth for base station applications," *IEEE Transactions on Antennas and Propagation*, vol. 68, pp. 4354-4361, 2020.

[9] H. H. Pennes, "Analysis of tissue and arterial blood temperatures in the resting human forearm," *Journal of Applied Physiology*, vol. 85, no. 1, pp. 5-34, 1998.

[10] G. Yildiz, T. Yilmaz, and I. Akduman, "Rotationally adjustable hyperthermia applicators: A computational comparative study of circular and linear array applicators," *Diagnostics*, vol. 12, no. 11, 2022, doi: 10.3390/diagnostics12112677.

[11] A. Khan, S. K. Dubey, and A. K. Singh, "Corner T-slot antenna at 2.45 GHz for hyperthermia application," *Journal of Electromagnetic Waves and Applications*, vol. 2024, pp. 1-14.

[12] R. M. Shehata, M. I. Badawi, and N. E. Ismail, "Hyperthermia for breast cancer treatment using a slotted microstrip patch antenna array," *Journal of Al-Azhar University Engineering Sector*, vol. 16, no. 61, pp. 1135-1155, 2021.

[13] M. R. Abdel-Haleem et al., "Enhancing microwave breast cancer hyperthermia therapy efficiency utilizing fat grafting with horn antenna," *International Journal of RF and Microwave Computer-Aided Engineering*, vol. 31, no. 6, 2021, e22651.

[14] M. Elsaadi and R. Hamad, "Breast cancer hyperthermia treatment based on slotted patch antenna at 2.45 GHz," *Circuits and Systems*, vol. 14, no. 5, pp. 10-18, 2023.

[15] K. R. Mahmoud and A. M. Montaser, "Design of multiresonance flexible antenna array applicator for breast cancer hyperthermia treatment," *IEEE Access*, vol. 10, pp. 93338-93352, 2022.